DOI: 10.1002/ejic.200901001

# A Selective Chromogenic and Fluorescent Molecular Probe for $Yb^{III}$ Based on a Bichromophoric Azadiene

**Fabiola Zapata,[a] Antonio Caballero,[a] Arturo Espinosa,[a] Alberto Tárraga,*[a] and Pedro Molina*[a]**

**Keywords:** Ytterbium / Azadienes / Ligand design / UV/Vis spectroscopy / Fluorescence

A new structurally simple motif, where two anthracene moieties are linked by a 2-aza-1,3-butadiene bridge has been synthesized and characterized. This new molecular probe senses $Yb^{3+}$ metal cations through two different channels: a colour change from yellowish to orange, which can be used for its "naked-eye" detection, and a remarkable enhancement in the fluorescence, even in the presence of other trivalent lanthanide metal cations.

## Introduction

The design of artificial molecular receptors for the selective detection of different target species is a topical field of supramolecular chemistry.[1] The intense research interest in this field is driven by the great demand for extremely sensitive and selective analytical tools able to recognize and sense environmentally and biologically important ionic species.[2]

Among the various detection techniques, fluorescent sensors make the best choice, as they are qualified with high sensitivity, high selectivity, fast response and inexpensive installations. One strategy employed in the design of chemosensors for metal cations is to link a fluorophore unit with a metal binding unit (ionophore). The two units are linked to each other in such a way that the binding of a cation to the ionophore causes considerable changes in the fluorescence of the fluorophore. Such changes can deal with intensity, intensity ratio, anisotropy, time-domain lifetime, phase modulation and so on.[3] To improve the fluorescence intensity enhancement of the receptor upon binding of metal cations one needs to carefully design the receptor molecule containing a fluorophore so that the responsible mechanism for fluorescence quenching is maximized in the receptor, whereas it is minimized in the metal-bound state of the receptor. For most of the fluorescent metal sensors described to date, this fluorescence modulation upon metal binding is commonly observed whenever a fluorophore interacts directly with a nonbonding electron pair belonging to a metal-chelating group, typically placed one or two bonds away from the fluorophore.[4]

A number of currently available fluorescent probes for metal cations actually change their fluorescent properties upon binding with such species. As fluorogenic groups, the anthryl substituent is very attractive because of its strong and well-characterized emissions and its chemical stability.[5]

On the other hand, trivalent lanthanides present a rich photophysical and coordination chemistry with important applications in both biology and medicine. Their growing interest has fortunately been highlighted in a number of recent reviews.[6] Whereas activity in this field was primarily focused on the use of complexes of Eu, Pr and Yb as shift reagents for NMR spectroscopy,[7] more recently, the interest has been focused on the development of new lanthanide(III)-containing systems used as molecular devices and in biomedical processes, such as nuclear magnetic imaging, cancer therapy, fluoroimmuno assays as well as specific cleavage of DNA and RNA.[8] In this context, it is also worth mentioning the emergent interest on the preparation and study of the physicochemical properties of complex chemical architectures containing one or more lanthanide(III) ions.[9]

Despite the fact that applications of lanthanide complexes is actually an active research theme, nowadays the synthesis of chemosensors for trivalent lanthanide ions is an attractive research field because there are only few reports about the design of selective chemosensors for these cations.[10] It has been reported that recognition of one specific lanthanide ion in the presence of others is a difficult challenge in view of the limited differences in chemical properties and size of these ions (0.18 Å between $La^{III}$ and $Lu^{III}$ and ca. 0.015 Å between two consecutive ions).[11]

[a] Departmento de Química Orgánica, Facultad de Química, Universidad de Murcia, Campus de Espinardo,
30100 Murcia, Spain
Fax: +34-868887499
E-mail: pmolina@um.es
atarraga@um.es

Supporting information for this article is available on the WWW under http://dx.doi.org/10.1002/ejic.200901001.

  

On the basis of this body of work, we have designed aza-substituted anthracene derivative **2**, which might be a suitable candidate for the selective sensing of this type of metal cation. In this receptor, the 2-aza-1,3-butadiene bridge, acting as both putative cation binding site and quencher of the fluorescence emission, is combined with the photoactive behaviour of the anthracene ring to endow the signalling properties. Thus, in this work we report the synthesis, characterization and metal cation coordination properties of 1,4-bis(9-anthryl)-2-aza-1,3-butadiene (**2**), in which two photoactive groups are directly attached by a 2-aza-1,3-butadiene bridge. The binding events involved in these recognitions processes are described by using UV/Vis, fluorescence and $^1$H NMR spectroscopy as well as by using theoretical calculations at the DFT level.

There are a few precedents of receptors[12] that combine a 2-aza-1,3-butadiene bridge as a putative cation binding site with the photoactivity of anthracene. However, in such cases another antenna moiety such as ferrocene is also directly linked to the azadiene bridge.[13] In this context, a ferrocene–anthracene dyad has been described[12a] for the selective $Li^+$ sensing in an aqueous environment, whose behaviour is based on the moderate basic character of the ferrocene moiety towards $Li^+$ cations.[14] Similarly, a triple chromogenic, fluorogenic and electrochemical $Zn^{2+}$ selective chemosensor has also been described that is based on a structural motif where two anthracene moieties are connected to a ferrocene subunit by two azadiene bridges.[12b]

## Results and Discussion

### Synthesis

Compound **2** was prepared following the recently described method for the synthesis of 1,4-disubstituted 2-aza-1,3-butadienes[15] (Scheme 1). Thus, readily available diethyl aminomethylphosphonate[16] was condensed with 9-anthracenecarboxaldehyde to give the corresponding *N*-substituted diethyl aminomethylphosphonate **1**[12a] in almost quantitative yield. Generation of the metalloenamine by reaction with *n*BuLi at –78 °C and subsequent reaction with 1 equivalent of the same aldehyde provided 1,4-bis(9-anthryl)-2-aza-1,3-butadiene (**2**), which was recrystallized from $CH_2Cl_2$/diethyl ether (1:10) and thoroughly characterized by using standard techniques: $^1$H and $^{13}$C NMR spectroscopy, mass spectrometry (ESI) as well as elemental analyses.

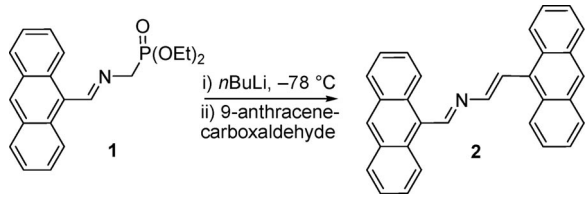


Scheme 1. Preparation of 1,4-bis(9-anthryl)-2-aza-1,3-butadiene (**2**).

Assignment of the (*E,E*) configuration of the double bonds present in azadiene derivative **2** was achieved by inspection of the $^1$H NMR spectroscopic data. It is well established that the condensation reaction between a primary amine and an aldehyde is not stereoselective; hence, both (*E*)- and (*Z*)-aldimine isomers are generally present in the reaction product. However, it must be emphasized that the condensation reaction between diethyl aminomethylphosphonate and 9-anthracenecarboxaldehyde takes place stereoselectively to give exclusively the (*E*)-isomer, as ascertained by NOE experiments. Indeed, an NOE effect is observed to the methylene group upon irradiation of the aldiminic proton of **1**. On the other hand, reaction of the deprotonated *N*-substituted diethyl aminophosphonates with 9-anthracenecarboxaldehyde gives only the *trans* configured carbon–carbon double bond, as is expected in a Horner–Wadsworth–Emmons olefination reaction, which is confirmed by the characteristic vicinal coupling constants obtained.

### Sensing Properties

The chemosensor behaviour of receptor **2** with several metal cations ($Li^+$, $Na^+$, $K^+$, $Mg^{2+}$, $Ca^{2+}$, $Ni^{2+}$, $Cu^{2+}$, $Zn^{2+}$, $Cd^{2+}$, $Hg^{2+}$, $Pb^{2+}$, $Sm^{3+}$, $Eu^{3+}$, $Gd^{3+}$, $Tb^{3+}$, $Yb^{3+}$ and $Lu^{3+}$)[17] in $CH_3CN$ was investigated by UV/Vis and fluorescence measurements, because this small system displays not only absorption but also emission variations depending on the metal ion present. All titrations experiments were analyzed by using a computer program.[18]

The UV/Vis spectrum of **2** in $CH_3CN$ exhibits the typical absorption bands of anthracene and its derivatives, as three shoulders at $\lambda$ = 348, 368 and 383 nm, along with an intense and broad low-energy (LE) band, centred at 420 nm, attributed to the aza bridge, which is responsible for the yellow colour of this receptor. Additionally, a very intense absorption band at $\lambda$ = 254 nm was also observed (see the Supporting Information). Titration experiments carried out by using the above-mentioned set of metal cations ($c$ = $2.5 \times 10^{-3}$ M in $CH_3CN$) demonstrate that host **2** can selectively recognize $Yb^{3+}$ and $Lu^{3+}$ because only those cations promote remarkable responses. A detailed UV/Vis analysis demonstrated that stepwise addition of such lanthanide cations induced the appearance of a new and weak low-energy band at $\lambda$ = 503 nm and $\lambda$ = 508 nm, respectively, (Table 1 and Figure 1) reaching its maximum in intensity when 1 equivalent of these lanthanide cations was added and which is responsible for the colour change from yellowish to orange and useful to be used for the "naked-eye" detection of these cations (see the Supporting Information). In each case, three well-defined isosbestic points were found during the titration experiments, indicating the presence of a unique complex in equilibrium with the neutral ligand.

The resulting Job's plots (see the Supporting Information) obtained during the titration processes clearly indicate a 1:1 binding model, the calculated association constants being $2.2 \times 10^4$ and $1.1 \times 10^4$ M$^{-1}$ for $Yb^{3+}$ and $Lu^{3+}$,

  

Table 1. UV/Vis and fluorescence data for compound **2** and for their corresponding metal complexes in $CH_3CN$.

| Compound | UV/Vis | Fluorescence | | $K_{as}$ [$M^{-1}$][e] | $D_{lim}$[f] |
|---|---|---|---|---|---|
| | $\lambda_{max}$ ($\varepsilon \times 10^{-3}$)[a] | $\lambda_{max}$[b] | $\phi$[c](CHEF)[d] | | |
| **2** | 420 (11.94) | 393, 416, 442 | $6.2 \times 10^{-4}$ | | |
| **2**·$Yb^{3+}$ | 423 (7.31), 503 (4.81) | 393, 414, 438, 467 | $2.1 \times 10^{-2}$ (125) | $5.6 \times 10^{4}$ | $5.7 \times 10^{-6}$ |
| **2**·$Lu^{3+}$ | 420 (10.61), 508 (4.80) | 393, 414, 438, 467 | $4.2 \times 10^{-3}$ (28) | $1.8 \times 10^{4}$ | $5.1 \times 10^{-6}$ |
| **2**·$Sm^{3+}$ | | 393, 414, 438, 467 | $1.8 \times 10^{-3}$ (16) | $1.7 \times 10^{4}$ | $4.2 \times 10^{-6}$ |
| **2**·$Eu^{3+}$ | | 393, 414, 438, 467 | $4.2 \times 10^{-3}$ (16) | $1.6 \times 10^{4}$ | $5.0 \times 10^{-6}$ |

[a] $\lambda_{max}$ in nm, $\varepsilon$ in $dm^3\,mol^{-1}\,cm^{-1}$. [b] $\lambda_{max}$ in nm. [c] See ref.[20] [d] CHEF = chelation-enhanced fluorescence effect. [e] Calculated from the fluorescence titration. [f] Detection limits.

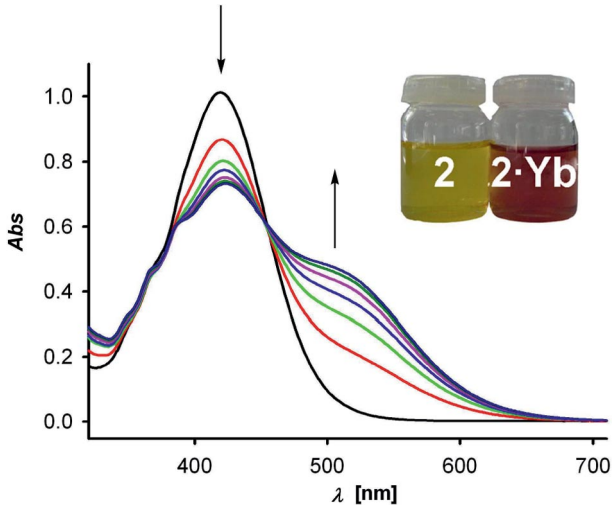


Figure 1. Changes in the absorption spectra of compound **2** (0.1 mM) in $CH_3CN$ upon addition $Yb^{3+}$ ion, from 0 (black) to 1 (purple) equivalent. Arrows indicate absorptions that increase or decrease during the experiment. Inset: changes in the colour of ligand **2** upon addition of $Yb^{3+}$ion.

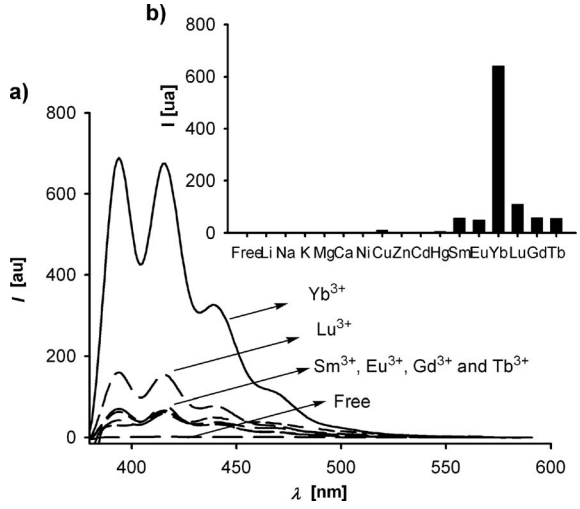


Figure 2. (a) Changes in the fluorescence emission spectrum of **2** ($c = 2.5 \times 10^{-5}$ M) in $CH_3CN$ upon addition of 1 equivalent of trivalent lanthanide metal cations ($c = 2.5 \times 10^{-3}$ M in $CH_3CN$); (b) fluorescence intensity increase for ligand **2**, in $CH_3CN$, in relation to the free ligand after addition of 1 equivalent of several cations. Emission is monitored at $\lambda_{exc}$ = 255 nm.

respectively. By contrast, addition of the above-mentioned alkali, alkali earth, transition-metal cations or other lanthanide ions studied ($Sm^{3+}$ and $Eu^{3+}$) resulted in no visible changes in the UV/Vis absorption spectrum.

The fluorescent spectral properties of ligand **2** ($c = 2.5 \times 10^{-5}$ M) were determined in $CH_3CN$ ($\lambda_{exc}$ = 255 nm), showing a very weak fluorescence ($\phi = 6.2 \times 10^{-4}$) and absence of the typical structured pattern of the parent anthracene. The low value of the quantum yield exhibited by the free ligand could be explained by an efficient quenching of the fluorescence, through a photoinduced electron transfer (PET) process, promoted by the N atom within the aza bridge.[19] However, when ligand **2** (Figure 2) was titrated with the above-mentioned trivalent lanthanide metal cations ($Sm^{3+}$, $Eu^{3+}$, $Yb^{3+}$ and $Lu^{3+}$), the well-structured anthracene-like spectrum was clearly observable, with four maxima at $\lambda$ = 393, 414, 438 and 467 nm. Nevertheless, it is worth mentioning that whereas the addition of 1 equivalent of $Sm^{3+}$, $Eu^{3+}$, $Gd^{3+}$, $Tb^{3+}$ and $Lu^{3+}$ promotes an almost-negligible increase in the chelation-enhanced fluorescent effect (CHEF) (Figure 2b), addition of $Yb^{3+}$ causes a 125-fold increase in CHEF and a 34-fold increase in the quantum yield[20] ($\phi = 2.1 \times 10^{-2}$; Table 1).

These data suggest that the coordination of the lanthanide metal ion with the N atom in the aza bridge is taking place so that the responsible PET mechanism for fluorescence quenching in the free ligand is minimized in its metal-bound state. The other tested alkali, alkaline earth and transition-metal ions showed no visible changes in the emission spectra. The stoichiometry of the complexes formed was also determined from the fluorescence titration data, which also indicate an empirical 1:1 stoichiometry, the estimated association constants and the calculated detection limits[21] being those collected in Table 1.

On the other hand, competition experiments performed between $Yb^{3+}$ and the other selected metal ions (see the Supporting Information) in $CH_3CN$ solution demonstrate that the emission spectra obtained displayed a pattern and intensity similar to that with $Yb^{3+}$ alone. Thus, this experimental results show that those metal cations do not have an obvious interfering effect on the fluorescence determination of $Yb^{3+}$.

For the reported constant to be taken with confidence, we proved the reversibility of the complexation process. If the sensing system is reversible, depletion of the cation that coordinates **2** must produce a change in either the absorp-

  

tion or emission spectrum, causing it to revert to the original spectrum. Formation of complex **2**·$Yb^{3+}$ or **2**·$Lu^{3+}$ and the subsequent decomplexation by extraction of the metal cation with ethylenediamine were carried out over several cycles. The optical and emission spectra were recorded after each step and found to be fully recovered upon completion of the step, thus demonstrating the high degree of reversibility of the sensing process (see the Supporting Information).

To gain a better understanding of the binding of receptor **2** to $Yb^{3+}$ and $Lu^{3+}$ ions, $^1$H NMR titration experiments were carried out. Figure 3 shows the spectra of **2** with different concentrations of $Yb^{3+}$. Significant downfield shifts were observed for the iminic (C*H*=N, $\Delta\delta$ = +0.20 ppm) and H-3′ ($\Delta\delta$ = +0.23 ppm) proton within the azadiene bridge (N–C*H*=CH, $\Delta\delta$ = +0.23 ppm), whereas the H-4′ in the bridge ($\delta$ = 7.76 ppm) and the H-1 proton of the anthracene moiety linked to the 1-position of the azadiene bridge are high shifted by $\Delta\delta$ = –0.11 ppm (N–CH=C*H*) and $\Delta\delta$ = –0.23 ppm, respectively.

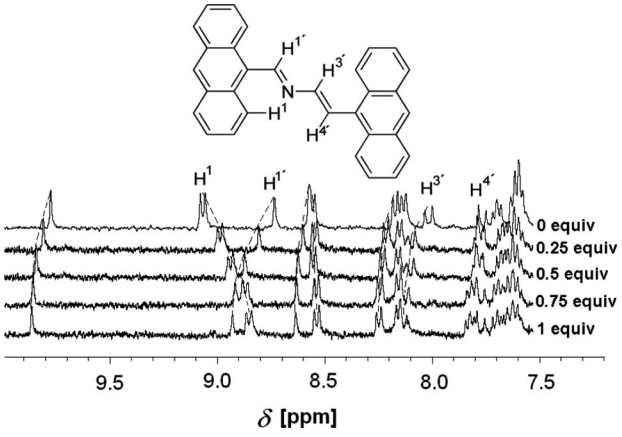


Figure 3. Evolution of the $^1$H NMR spectra of **2** (top) upon addition of increasing amounts of $Yb^{3+}$ until 1 equivalent was added (bottom).

The nature of the complexes formed has also been studied by electrospray mass spectrometry (MS-ESI) of the isolated solid complexes, because all attempts to obtain suitable crystals for X-ray analysis were unsuccessful. This result confirms a real [1+1] nature stoichiometry for such complexes (see the Supporting Information). Thus, peaks at *m*/*z* = 878 and *m*/*z* = 880 indicate the presence of the fragments [**2**·$Yb(OTf)_2$]$^+$ and [**2**·$Lu(OTf)_2$]$^+$, respectively (see the Supporting Information).

Binding of trivalent lanthanide ions by simple receptor **2** was also investigated by quantum chemical calculations. The observed selectivity of ligand **2** towards $Yb^{3+}$ in comparison to the other metal cations (as their triflate salts) was initially studied at the semiempirical level of theory by using the PM6 Hamiltonian.[22] The structure of complex [**2**·$Ln(OTf)_3$] (Ln: Lu, Yb) was then refined at the DFT level of theory. Due to the open-shell nature of the $Yb^{3+}$-containing complexes, first the structure for the [**2**·$Lu(OTf)_3$] complex was calculated by following the experimentally observed 1:1 ligand/cation ratio, its free energy of formation (in MeCN solution) being –12.79 kcal mol$^{-1}$. The resulting geometry was then used as a starting point for the optimization of the – quantitatively – more interesting [**2**·$Yb(OTf)_3$] complex, whose absolute minimum structure (Figure 4) shows the $Yb^{3+}$ metal ion bonded to the azadiene N atom ($d_{N\cdots Yb}$ = 2.540 Å, $WBI_{N\cdots Yb}$ = 0.071) and featuring a weak but significant interaction with the C-1 atom of the closest anthryl unit ($d_{C\cdots Yb}$ = 2.847 Å, $WBI_{C\cdots Yb}$ = 0.031) as unambiguously proved by location of the corresponding bond critical point [$\rho(r_c) = 1.82\times10^{-2}$ e $a_0^{-3}$; $\nabla^2\rho(r_c) = 6.32\times10^{-2}$ e $a_0^{-5}$]. The hexacoordination sphere around $Yb^{3+}$ is completed by four O donor atoms belonging to three triflate units (range $d_{O\cdots Yb}$ = 2.210–2.387 Å, $WBI_{O\cdots Yb}$ = 0.114–0.091). One of these O atoms simultaneously forms a weak hydrogen bond to azadiene H-4′ [range $d_{O\cdots H4'}$ = 2.598 Å, $WBI_{O\cdots H3'}$ = 0.005; $\rho(r_c) = 0.89\times10^{-2}$ e $a_0^{-3}$; $\nabla^2\rho(r_c) = 2.61\times10^{-2}$ e $a_0^{-5}$] that explains the observed downfield shift for the corresponding signal in the $^1$H NMR spectra.

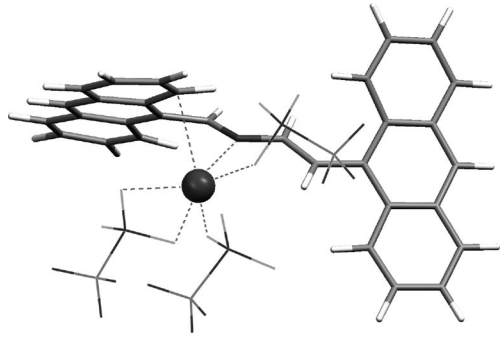

Figure 4. Calculated (mPW1B95/aug6-311G**/StRSC-ecp) structure for the complex [**2**·$Yb(OTf)_3$]. Triflate ligands are displayed in wireframe for clarity.

## Conclusions

Here we report on the preparation of a simple and easy-to-make new chemosensor **2** based on two anthracene subunits linked by a 2-aza-1,3-butadiene bridge and which can operate through absorption and emission channels in acetonitrile solutions. Receptor **2** exhibits significant changes in its UV/Vis spectrum in the presence of both $Lu^{3+}$ and $Yb^{3+}$, which can be used for the naked-eye detection of these metal cations. On the other hand, this receptor selectively senses $Yb^{3+}$ when emission spectroscopy was used. This versatile receptor represents an interesting highly selective fluorescent sensor for $Yb^{3+}$ in the presence of other lanthanide cations.

## Experimental Section

**General Methods:** The starting material 9-antracenecarboxaldehyde was purchased from Sigma–Aldrich and used as received. Solvents were analytical-grade quality and were purified by standard procedures before use. Counteranion for the $Li^+$, $Na^+$, $K^+$, $Mg^{2+}$, $Ca^{2+}$, $Ni^{2+}$, $Cd^{2+}$, $Hg^{2+}$ and $Pb^{2+}$ metal cations was perchlorate,

  

whereas $Cu^{2+}$, $Zn^{2+}$, $Sm^{3+}$, $Eu^{3+}$, $Gd^{3+}$, $Tb^{3+}$, $Yb^{3+}$ and $Lu^{3+}$ were used as their trifluoromethanesulfonate salts. Melting points were determined with a Kofler hot plate melting point apparatus and are uncorrected. Elemental analyses were carried out with a Carlo–Erba EA-1108 analyzer. $^1H$ and $^{13}C$ NMR spectra were recorded at 400 and 100 MHz, respectively, with a Bruker AC400 apparatus at 25 °C. Chemical shifts refer to signals of tetramethylsilane in the case of $^1H$ and $^{13}C$ spectra. The following abbreviations are used to represent the multiplicity of the signals: s (singlet), d (doublet) and q (quaternary carbon atom). ESI mass spectra were recorded with a Fisons AUTOSPEC 500 VG spectrometer. UV/Vis spectra were carried out with a UV/Vis Varian 5000 spectrophotometer by using a dissolution cell of 10-mm path. The samples were dissolved in $CH_3CN$ ($c = 1\times10^{-4}$ M), and the spectra were recorded with the spectra background corrected before and after the sequential addition of aliquots of 0.1 equivalent of $M^{2+}$ in the same solvent ($c = 2.5\times10^{-2}$ M). Fluorescence spectra were carried out with a Varian Carey fluorescence spectrophotometer by using a 10-mm fluorescence cell ($c = 2.5\times10^{-5}$ M), as it is stated in the corresponding figure captions. Before recording the spectra, the samples were deoxygenated to remove fluorescence quenching by oxygen by bubbling nitrogen for at least 10 min All the spectra were recorded before and after the sequential additions of aliquots of 0.1 equivalent of a solution of $M^{2+}$ in $CH_3CN$ ($c = 2.5\times10^{-3}$ M). Quantum yield values were measured with respect to anthracene as standard ($\Phi = 0.27\pm0.01$) by using the equation $\Phi_x/\Phi_s = (S_x/S_s)\,[(1-10^{-A_s})/(1-10^{-A_x})](n_s^2/n_x^2)$, where $x$ and s indicate the unknown and standard solution, respectively, $\Phi$ is the quantum yield, $S$ is the area under the emission curve and $A$ is the absorbance at the excitation wavelength and $n$ is the index of refraction. Competition experiments were carried out by addition of 0.5 equivalent of selected metal ions ($c = 2.5\times10^{-3}$) to a $CH_3CN$ solution of **2** ($c = 2.5\times10^{-5}$) containing 0.5 equivalent of $Yb^{3+}$ ($c = 2.5\times10^{-3}$). All these experiments were carried out at 25 °C.

**Preparation of 1,4-Bis(9-anthryl)-2-aza-1,3-butadiene (2):** To a solution of **1** (0.77 g, 4.64 mmol) in dry THF (20 mL) at 78 °C and under a nitrogen atmosphere was added the adequate amount of *n*BuLi (1.6 M in hexane). Then, a solution of 9-anthracenecarboxaldehyde (0.96 g, 4.64 mmol) in dry THF (10 mL) was added dropwise, and the solution was stirred for 1.5 h. The reaction mixture was allowed to reach room temperature, and afterwards, it was heated under reflux temperature overnight. After the solution was cooled to room temperature, the solvent was evaporated under reduced pressure, and the resulting solid was slurried with diethyl ether (25 mL) to give a crude product that was recrystallized from dichloromethane/diethyl ether (1:10). Yield: 85% (1.80 g). M.p. 247–248 °C. $^1H$ NMR (400 MHz, $CDCl_3$, 25 °C): $\delta$ = 7.63–7.57 (m, 6 H), 7.71–7.68 (m, 2 H), 7.76 (d, $^3J_{H,H}$ = 13.2 Hz, 1 H, -*N*-CH=C*H*-), 8.01 (d, $^3J_{H,H}$ = 13.2 Hz, 1 H, -*N*-C*H*=CH-), 8.13 (d, $^3J_{H,H}$ = 8.4 Hz, 2 H), 8.16 (d, $^3J_{H,H}$ = 8.4 Hz, 2 H), 8.55 (d, $^3J_{H,H}$ = 8.8 Hz, 2 H), 8.57 (s, 1 H), 8.73 (s, 1 H, -C*H*=N-), 9.06 (d, $^3J_{H,H}$ = 8.8 Hz, 2 H), 9.77 (s, 1 H) ppm. $^{13}C$ NMR (100 MHz, $CDCl_3$, 25 °C): $\delta$ = 124.9 (-*N*-CH=*C*H-), 125.3 (CH), 125.5 (CH), 125.7 (CH), 126.1 (CH), 126.7 (q), 126.9 (CH), 127.4 (CH), 127.7 (CH), 128.8 (CH), 129.1 (CH), 130.0 (q), 130.6 (q), 130.9 (q), 131.0 (CH), 131.4 (q), 131.5 (q), 149.7 (N-*C*H=CH), 160.8 (*C*H=N) ppm. MS (ESI, 70 eV): *m*/*z* (%) = 407 (100) [$M^+$], 229 (13), 216 (10), 204 (53), 202 (42), 191 (27), 178 (13). $C_{31}H_{21}N$ (407.17): calcd. C 91.37, H 5.19, N 3.44; found C 91.48, H 5.31, N 3.27.

**Computational Details:** Initial geometries and energies for all complexes and free ligands were obtained at the semiempirical level of theory by using the PM6 Hamiltonian and the Mopac2007 software.[23] Solvent (acetonitrile) effects were taken into account by the Conductor-like Screening Model (COSMO) method[24] by using 36.64 as relative static permittivity of the solvent and conducting polygonal surfaces around every atom at the van der Waals' distances made up of 162 segments each. The reliably accurate description of weak interactions like hydrogen bonds (HBs) and other found in supramolecular complexes generally requires a treatment of electron correlation. Density functional theory[25] (DFT) proved quite useful in this regard for studying systems with HBs,[26] offering an electron correlation correction frequently comparable to the second-order Møller–Plesset theory (MP2) or in certain cases, and for certain purposes, even superior to MP2, but at considerably lower computational cost. Calculated geometries at the DFT level were fully optimized in the gas phase with tight convergence criteria by using the Gaussian 03 package,[27] employing the hybrid meta functional mPW1B95[28] that has been recommended for general purpose applications and was developed to produce a better performance where weak interactions are involved, such as those between ligands and heavy metals.[29] Due to the size of the systems investigated in the present study the cost advantage that offers mPW1B95 method in comparison with MP2 was significant. The 6-311G** basis set was used in the optimizations for all atoms and adding diffuse functions on N, O and F atoms (denoted as aug6-311G**), as well as the Stuttgart relativistic small-core basis set (StRSC) with effective core potential (ecp) for ytterbium and lutetium.[30] From these gas-phase-optimized geometries all reported data were obtained by means of single-point (SP) calculations at the aug6-311G**/StRSC-ecp level. Energy values are uncorrected for the zero-point vibrational energy and were computed considering solvent (acetonitrile) effects by using the Cossi and Barone's CPCM (conductor-like polarizable continuum model) modification[31] of the Tomasi's PCM formalism[32] and correcting the basis set superposition error (BSSE) by means of the counterpoise approach.[33] Bond orders were characterized by the Wiberg's bond index[34] (WBI) and calculated with the natural bond orbital (NBO) method as the sum of squares of the off-diagonal density matrix elements between atoms. The topological analysis of the electronic charge density was conducted by means of the Bader's AIM methodology[35] by using the AIM2000 software[36] and the wavefunction at the working level of theory.

**Supporting Information** (see footnote on the first page of this article): $^1H$ and $^{13}C$ NMR spectra of ligand **2**; UV/Vis and fluorescence titration experiments; Job's plots; competition and reversibility experiments; ESI mass spectra; Cartesian coordinates; energies for **2** and its complexes.

## Acknowledgments

We gratefully acknowledge financial support from Ministerio de Ciencia e Innovación (MICINN) – Spain, Project CTQ2008-01402 and Fundación Séneca (Agencia de Ciencia y Tecnología de la Región de Murcia) project 04509/GERM/06 (Programa de Ayudas a Grupos de Excelencia de la Región de Murcia, Plan Regional de Ciencia y Tecnología 2007/2010). A. C. also thanks the Ministerio de Educación y Ciencia for a predoctoral grant.

[1] a) J.-M. Lehn, *Supramolecular Chemistry*, VCH, New York, **1995**; b) A. W. Czarnik, *Chem. Biol.* **1995**, *2*, 423–428; c) J. L. Atwood, J. E. D. Davis, D. D. McNicol, F. Vögtle, J.-M. Lehn (Eds.), *Comprehensive Supramolecular Chemistry*, Pergamon, Oxford, UK, **1996**, vols. 1–11; d) T. Schrader, A. Hamilton, *Functional Synthetic Receptors*, Wiley, New York, **2005**; e) E. V. Anslyn, *J. Org. Chem.* **2007**, *72*, 687–699.

  

[2] a) U. E. Spichiger-Keller, *Chemical Sensors and Biosensors for Medical and Biological Applications*, Wiley-VCH, Weinheim, **1998**; b) R. P. Haugland, *Handbook of Fluorescent Probes and Research Products*, 8th ed., Molecular Probes, Eugene, OR, **2001**.

[3] a) J. R. Lakowicz (Ed.), *Topics in Fluorescence Spectroscopy*, Plenum Press, New York, **1994**; b) J. R. Lakowicz, *Principles of Fluorescence Spectroscopy*, Kluwer Academic/Plenum Publishers, New York, **1999**; c) B. Valeur, *Molecular Fluorescence*, Wiley-VCH, Weinheim, **2001**; d) Special Issue on Fluorescent Sensors: A. P. de Silva, P. Tecilla (Guest Eds.), *J. Mater. Chem.* **2005**, *15*, 2617–2976.

[4] a) A. P. de Silva, H. Q. N. Gunaratne, T. Gunnlaugsson, A. J. M. Huxley, C. P. McCoy, J. T. Rademacher, T. E. Rice, *Chem. Rev.* **1997**, *97*, 1515–1566; b) J. P. Desvergne, A. W. Czarnik (Eds.), *Fluorescent Chemosensors for Ion and Molecule Recognition*, Kluwer Academic Publishers, Dordrecht, The Netherlands, **1997**; c) L. Prodi, F. Bolletta, M. Montalti, N. Zaccheroni, *Coord. Chem. Rev.* **2000**, *205*, 59–83; d) B. Valeur, I. Leray, *Coord. Chem. Rev.* **2000**, *205*, 3–40; e) A. P. de Silva, D. B. Fox, A. J. M. Huxley, T. S. Moody, *Coord. Chem. Rev.* **2000**, *205*, 41–57; f) D. Parker, R. S. Dickins, H. Puschmann, C. Cossland, J. A. K. Howard, *Chem. Rev.* **2002**, *102*, 1977–2010; g) J. F. Callan, A. P. de Silva, D. C. Magri, *Tetrahedron* **2005**, *61*, 8551–8588; h) L. Prodi, *New J. Chem.* **2005**, *29*, 20–31.

[5] a) A. P. de Silva, S. A. de Silva, *J. Chem. Soc., Chem. Commun.* **1986**, 1709–1710; b) A. P. de Silva, H. Q. Gunaratne, C. P. McCoy, *Chem. Commun.* **1996**, 2399–2400; c) A. P. de Silva, H. Q. N. Gunaratne, T. Gunnlaugsson, A. J. M. Huxley, C. P. McCoy, J. T. Rademacher, T. E. Rice, *Chem. Rev.* **1997**, *97*, 1515–1566; d) T. Gunnlaugsson, A. P. Davis, M. Glynn, *Chem. Commun.* **2001**, 2556–2557; e) G. W. Gokel, W. M. Leevy, M. E. Weber, *Chem. Rev.* **2004**, *104*, 2723–2750; f) S. J. Brooks, C. Caltagirone, A. J. Cossins, P. A. Gale, M. Light, *Supramol. Chem.* **2008**, *20*, 349–355; g) Y. Kohno, Y. Shiraishi, T. Hirai, *J. Photochem. Photobiol. A: Chem.* **2008**, *195*, 267–276; h) K. Ghosh, A. R. Sarkar, *Tetrahedron Lett.* **2009**, *50*, 85–88.

[6] a) C. Piguet, J.-C. G. Bünzli, *Chem. Soc. Rev.* **1999**, *28*, 347–358; b) D. Parker, *Coord. Chem. Rev.* **2000**, *205*, 109–130; c) Special Issue on Frontiers in Lanthanide Chemistry: H. B. Kagan (Guest Ed.), *Chem. Rev.* **2002**, *102*, 1805–2476; d) M. Woods, Z. Kovacs, A. D. Sherry, *J. Supramol. Chem.* **2002**, *2*, 1–15; e) D. Parker, *Chem. Soc. Rev.* **2004**, *33*, 156–165; f) . T. Gunnlaugsson, J. P. Leonard, *Chem. Commun.* **2005**, 3114–3131; g) J. P. Leonard, T. Gunnlaugsson, *J. Fluoresc.* **2005**, *15*, 585–595; h) T. Gunnlaugsson, F. Stomeo, *Org. Biomol. Chem.* **2007**, *5*, 1999–2009; i) C. M. G. dos Santos, A. J. Harte, S. J. Quinn, T. Gunnlaugsson, *Coord. Chem. Rev.* **2008**, *252*, 2512–2527; j) J. Shen, L.-D. Sun, C.-H. Yan, *Dalton Trans.* **2008**, 5687–5697; k) A. Thibon, V. C. Pierre, *Anal. Bioanal. Chem.* **2009**, *394*, 107–120.

[7] J. H. Forsberg in *Handbook on the Physics and Chemistry of Rare Earths* (Eds.: J. K. A. Gschneidner, L. Eyring), Elsevier, Amsterdam. **1966**, vol. 23, pp. 1–68.

[8] a) J.-C. G Bünzli, G. R. Choppin in *Lanthanide Probes in Life. Chemical and Earth Sciences* (Eds.: J.-C. G Bünzli, G. R. Choppin), Elsevier, Amsterdam, **1989**; b) C. H. Evans, *Biochemistry of the Lanthanides*, Plenum, New York, **1990**; c) A. E. Merbach, E. Tóth, *The Chemistry of Contrast Agents in Medical Magnetic Resonance Imaging*, Wiley, New York, **2001**.

[9] a) D. Chapon, P. Delangle, C. Lebrun, *J. Chem. Soc., Dalton Trans.* **2002**, 68–74; b) I. Oueslati, R. A. Sá Ferreira, L. D. Carlos, C. Baleizao, M. N. Berberan-Santos, B. de Castro, J. Vicens, U. Pischel, *Inorg. Chem.* **2006**, *45*, 2652–2660; c) G. Canard, S. Koeller, G. Bernardinelli, C. Piguet, *J. Am. Chem. Soc.* **2008**, *130*, 1025–1040; d) T. B. Jensen, R. Scopelliti, J.-C. G. Bünzli, *Dalton Trans.* **2008**, 1027–1036; e) W. Huang, D. Wu, D. Guo, X. Zhu, C. He, Q. Meng, C. Duan, *Dalton Trans.* **2009**, 2081–2084; f) P. Kadjane, M. Starck, F. Camerel, F. Hill, N. Hildebrandt, R. Ziessel, L. J. Charbonnière, *Inorg. Chem.* **2009**, *48*, 4601–4603; g) S. Faulkner, L. S. Natrajan, W. S. Perry, D. Sykes, *Dalton Trans.* **2009**, 3890–3899.

[10] a) T. Gunnlaugsson, *Tetrahedron Lett.* **2001**, *42*, 8901–8905; b) G. D. Brindley, O. D. Fox, P. D. Beer, *J. Chem. Soc., Dalton Trans.* **2000**, 4354–4359; c) V. Bekiari, P. Judeinstein, P. Lianos, *J. Lumin.* **2003**, *104*, 13–15; d) Z. Liu, L. Jiang, Z. Liang, Y. Gao, *Tetrahedron* **2006**, *62*, 3214–3220; e) I. Oueslati, R. A. Sa Ferreira, L. D. Carlos, C. Balezao, M. N. Berberan-Santos, B. de Castro, J. Vicens, U. Pischel, *Inorg. Chem.* **2006**, *45*, 2652–2660; f) Z. Liang, Z. Liu, Y. Gao, *Tetrahedron Lett.* **2007**, *48*, 3587–3590.

[11] N. André, T. B. Jemsem, R. Scopelliti, D. Imbert, M. Elhabiri, G. Hopfgartner, C. Piguet, J.-C. G. Bünzli, *Inorg. Chem.* **2004**, *43*, 515–529.

[12] a) A. Caballero, R. Tormos, A. Espinosa, M. D. Velasco, A. Tárraga, M. A. Miranda, P. Molina, *Org. Lett.* **2004**, *6*, 4599–4602; b) F. Zapata, A. Caballero, A. Espinosa, A. Tárraga, P. Molina, *Org. Lett.* **2007**, *9*, 2385–2388.

[13] P. Molina, A. Tárraga, A. Caballero, *Eur. J. Inorg. Chem.* **2008**, 3401–3417.

[14] a) P. Burk, I. A. Koppel, I. Koppel, R. Kurg, J.-F. Gal, P.-C. Maria, M. Herreros, R. Notario, J.-L. M. Abboud, I. Anvia, R. F. Taft, *J. Phys. Chem. A* **2000**, *40*, 1424–1427; b) A. Irigoras, J. M. Mercero, I. Silanes, J. M. Ugalde, *J. Am. Chem. Soc.* **2001**, *123*, 5040–5043; c) J. Rodríguez-Otero, E. M. Cabaleiro-Lago, A. Peña-Gallego, M. M. Montero-Campillo, *Tetrahedron* **2009**, *65*, 2368–2371.

[15] V. Lloveras, A. Caballero, A. Tárraga, M. D. Velasco, A. Espinosa, K. Wurst, D. J. Evans, J. Vidal-Gancedo, C. Rovira, P. Molina, J. Veciana, *Eur. J. Inorg. Chem.* **2005**, 2436–2450.

[16] S. K. Davidsen, G. W. Phillips, S. F. Martin, *Org. Synth.* **1993**, *8*, 451–458.

[17] $Li^+$, $Na^+$, $K^+$, $Mg^{2+}$, $Ca^{2+}$, $Ni^{2+}$, $Cd^{2+}$, $Hg^{2+}$ and $Pb^{2+}$ were used as their perchlorate salts, whereas $Cu^{2+}$, $Zn^{2+}$, $Sm^{3+}$, $Eu^{3+}$, $Gd^{3+}$, $Tb^{3+}$, $Yb^{3+}$ and $Lu^{3+}$ were used as their trifluoromethanesulfonate salts.

[18] *Specfit/32 Global Analysis System*, 1999–2004, Spectrum Software Associates (SpecSoft@compuserve.com).

[19] R. Martínez, F. Zapata, A. Caballero, A. Espinosa, A. Tárraga, P. Molina, *Org. Lett.* **2006**, *8*, 3235–3238.

[20] The fluorescence quantum yields were measured with respect to anthracene as standard ($\Phi$ = 0.27). W. R. Dawson, M. W. Windsor, *J. Phys. Chem.* **1968**, *72*, 3251–3260.

[21] M. Shortreed, R. Kopelman, M. Kuhn, B. Hoyland, *Anal. Chem.* **1996**, *68*, 1414–1418.

[22] J. J. P. Stewart, *J. Mol. Model.* **2007**, *13*, 1173–1213.

[23] *MOPAC2007*, J. J. P. Stewart, Stewart Computational Chemistry, Colorado Springs, CO, USA, http://OpenMOPAC.net (**2007**).

[24] A. Klamt, G. Schüürmann, *J. Chem. Soc. Perkin Trans. 2* **1993**, 799–805.

[25] a) A. D. Becke, *J. Chem. Phys.* **1993**, *98*, 5648–5652; b) C. Lee, W. Yang, R. G. Parr, *Phys. Rev. B* **1998**, *37*, 785–789; c) S. H. Vosko, L. Wilk, M. Nusair, *Can. J. Phys.* **1980**, *58*, 1200–1211; d) P. J. Stephens, F. J. Devlin, C. F. Chabalowskin, M. J. Frisch, *J. Phys. Chem.* **1994**, *98*, 11623–11627.

[26] P. R. Rablen, J. W. Lockman, W. L. Jorgensen, *J. Phys. Chem. A* **1998**, *102*, 3782–3797.

[27] M. J. Frisch, G. W. Trucks, H. B. Schlegel, G. E. Scuseria, M. A. Robb, J. R. Cheeseman, J. A. Montgomery Jr., T. Vreven, K. N. Kudin, J. C. Burant, J. M. Millam, S. S. Iyengar, J. Tomasi, V. Barone, B. Mennucci, M. Cossi, G. Scalmani, N. Rega, G. A. Petersson, H. Nakatsuji, M. Hada, M. Ehara, K. Toyota, R. Fukuda, J. Hasegawa, M. Ishida, T. Nakajima, Y. Honda, O. Kitao, H. Nakai, M. Klene, X. Li, J. E. Knox, H. P. Hratchian, J. B. Cross, V. Bakken, C. Adamo, J. Jaramillo, R. Gomperts, R. E. Stratmann, O. Yazyev, A. J. Austin, R. Cammi, C. Pomelli, J. W. Ochterski, P. Y. Ayala, K. Morokuma, G. A. Voth, P. Salvador, J. J. Dannenberg, V. G. Zakrzew-

  

ski, S. Dapprich, A. D. Daniels, M. C. Strain, O. Farkas, D. K. Malick, A. D. Rabuck, K. Raghavachari, J. B. Foresman, J. V. Ortiz, Q. Cui, A. G. Baboul, S. Clifford, J. Cioslowski, B. B. Stefanov, G. Liu, A. Liashenko, P. Piskorz, I. Komaromi, R. L. Martin, D. J. Fox, T. Keith, M. A. Al-Laham, C. Y. Peng, A. Nanayakkara, M. Challacombe, P. M. W. Gill, B. Johnson, W. Chen, M. W. Wong, C. Gonzalez, J. A. Pople, *Gaussian 03*, Revision B.03, Gaussian, Inc., Wallingford, CT, **2004**.

[28] a) Y. Zhao, D. G. Truhlar, *J. Phys. Chem. A* **2004**, *108*, 6908–6918; b) Y. Zhao, D. G. Truhlar, *J. Phys. Chem. A* **2005**, *109*, 5656–5667.

[29] For instance, see: J. Muñiz, L. E. Sansores, A. Martínez, R. Salcedo, *J. Mol. Struct.* **2007**, *820*, 141–147.

[30] The Stuttgart relativistic small core basis set were obtained from The Basis Set Exchange (BSE) version 1.2.2, as developed and distributed by the Environmental Molecular Sciences Laboratory: K. L. Schuchardt, B. T. Didier, T. Elsethagen, L. Sun, V. Gurumoorthi, J. Chase, J. Li, T. L. Windus, *J. Chem. Inf. Model.* **2007**, *47*, 1045–1052, https://bse.pnl.gov/bse/portal.

[31] a) V. Barone, M. Cossi, *J. Phys. Chem. A* **1998**, *102*, 1995–2001; b) M. Cossi, N. Rega, G. Scalmani, V. Barone, *J. Comput. Chem.* **2003**, *24*, 669–681.

[32] a) S. Miertus, E. Scrocco, J. Tomasi, *Chem. Phys.* **1981**, *55*, 117–129; b) R. Cammi, B. Mennucci, J. Tomasi, *J. Phys. Chem. A* **2000**, *104*, 5631–5637.

[33] S. F. Boys, F. Bernardi, *Mol. Phys.* **1970**, *19*, 553–566.

[34] K. Wiberg, *Tetrahedron* **1968**, *24*, 1083–1096.

[35] R. F. W Bader, *Atoms in Molecules: A Quantum Theory*, Oxford University Press, Oxford, **1990**.

[36] a) AIM2000 v. 2.0, designed by F. W. Biegler-König, J. Schönbohm, **2002**, homepage http://www.aim2000.de/; F. Biegler-König, J. Schönbohm, D. J. Bayles, *Comput. Chem.* **2001**, *22*, 545–559; b) F. Biegler-König, J. Schönbohm, *J. Comput. Chem.* **2002**, *23*, 1489–1494.

Received: October 13, 2009
Published Online: Decembrer 18, 2009

  